

Published in final edited form as:

Dev Dyn. 2010 February ; 239(2): 548–558. doi:10.1002/dvdy.22201.

Churchill and Sip1a repress FGF signaling during zebrafish somitogenesis

Fatma O. Kok^{1,2}, Iain T. Shepherd³, and Howard I. Sirotkin¹

¹Department of Neurobiology and Behavior, Stony Brook University, Stony Brook NY.

²Graduate Program in Molecular and Cellular Biology, Stony Brook University, Stony Brook, NY

³Department of Biology, Emory University, Atlanta, GA.

Abstract

Cell-type specific regulation of a small number of growth factor signal transduction pathways generates diverse developmental outcomes. The zinc finger protein Churchill (ChCh) is a key effector of Fibroblast Growth Factor (FGF) signaling during gastrulation. ChCh is largely thought to act by inducing expression of the multifunctional Sip1 (Smad Interacting Protein 1). We investigated the function of ChCh and Sip1a during zebrafish somitogenesis. Knockdown of ChCh or Sip1a results in misshapen somites that are short and narrow. As in wild-type embryos, cycling gene expression occurs in the developing somites in ChCh and Sip1a compromised embryos, but expression of *her1* and *her7* is maintained in formed somites. In addition, tailbud *fgf8* expression is expanded anteriorly in these embryos. Finally, we found that blocking FGF8 restores somite morphology in ChCh and Sip1a compromised embryos. These results demonstrate a novel role for ChCh and Sip1a in repression of FGF activity.

Introduction

Fibroblast growth factors (FGFs) play essential roles in cell growth and differentiation in many developmental contexts (Amaya et al., 1991; Sutherland et al., 1996; Borland et al., 2001; Coumoul and Deng, 2003; Furthauer et al., 2004; Bottcher and Niehrs, 2005; Thisse and Thisse, 2005; Huang et al., 2007; Krens et al., 2008). During vertebrate embryogenesis, FGFs are required for induction of both mesoderm and neural ectoderm, patterning of the midbrain, posteriorization of the neural plate and segmentation of the mesoderm. In vertebrates, the FGF family contains over 20 ligands that interact with four receptors. The mechanisms that account for the diverse responses evoked by FGFs have yet to be fully elucidated, but depend on cell-type specific modulators of signaling.

One such FGF effector is the zinc finger protein Churchill (ChCh), which regulates FGF activity during gastrulation. ChCh is slowly induced in response to FGF and acts as a switch between mesoderm and neural inducing activities of FGF in chick, *Xenopus* and zebrafish (Sheng et al., 2003; Snir et al., 2006; Londin et al., 2007a). ChCh inhibits expression of mesodermal markers including *brachyury*, *Tbx6L*, and *spt* and blocks mesoderm induction, which requires FGF signaling in cooperation with Activin/Nodal activity (Kimelman and Maas, 1992; LaBonne and Whitman, 1994). ChCh also regulates cell movements during gastrulation. In the chick, ChCh blocks ingression of presumptive ectoderm through the primitive streak at the end of gastrulation. Therefore, these cells adopt

neural fates instead of ingressing through the streak and becoming paraxial mesoderm (Sheng et al., 2003). Similarly, when zebrafish blastomeres with compromised ChCh activity are transplanted to the animal pole of wild type hosts, they leave the epiblast, migrate to the germ ring and acquire mesodermal fates (Londin et al., 2007b).

ChCh was initially thought to regulate transcription of target genes via a direct DNA interaction. However, subsequent biophysical characterization of ChCh has suggested that it may not be a DNA binding protein (Lee et al., 2007). None-the-less, by direct or indirect mechanisms, ChCh induces *sip1* (Smad Interacting Protein 1) transcription (Sheng et al., 2003; Snir et al., 2006; Londin et al., 2007a), which is key to the activity of ChCh. Sip1 is a multifunctional molecule that modulates TGF- β signaling by converting activated forms of both Smad1/5 and Smad2/3 to transcriptional repressors (Remacle et al., 1999; Verschuere et al., 1999; Postigo, 2003; Postigo et al., 2003). In addition, Sip1 regulates cell movements by directly repressing E-cadherin transcription (Remacle et al., 1999; Comijn et al., 2001) and mesoderm induction by directly impeding *Xbra* transcription (Remacle et al., 1999; Verschuere et al., 1999).

In zebrafish, *chch* is expressed after gastrulation (Londin et al., 2007a), but later roles for ChCh have not been studied. We now present data that ChCh and Sip1 are required for somitogenesis. Segmentation is an essential step in formation of the vertebrate body axis. Mesodermal segmentation is established by sequentially dividing the unsegmented presomitic mesoderm into the bilaterally segmented structures called somites. The “clock and wavefront” model describes the mechanisms of regulation of somitogenesis (Cooke, 1978; Palmeirim et al., 1997; Forsberg et al., 1998; McGrew et al., 1998; Jiang et al., 2000; Bessho et al., 2001; Saga and Takeda, 2001). In zebrafish, the “clock and wavefront” model proposes that function of a molecular oscillator in the presomitic mesoderm (PSM) results in controlled expression of a set of genes associated with the Notch pathway (Holley et al., 2000; Jiang et al., 2000; Pourquie, 2001; Pourquie, 2003). Simultaneously, the wavefront modulates the ability of the PSM to respond to the morphogenic signals and produce segments (Cooke and Zeeman, 1976; Dale and Pourquie, 2000; Giudicelli and Lewis, 2004). The pulses generated by the molecular clock are translated into very highly regulated spatial periodicity. Despite the similarities in somitogenesis between species, there are differences between amniotes and mammals in the segmentation program (Giudicelli and Lewis, 2004; Cinquin, 2007). For example, *lunatic fringe* and *delta* genes appear to function differently in mouse, chick and zebrafish (Prince et al., 2001; Sato et al., 2002; Dale et al., 2003; Serth et al., 2003; Qiu et al., 2004). In addition, the Wnt pathway is important for regulation of segmentation clock in mice (Takada et al., 1994; Aulehla et al., 2003), but not zebrafish.

Previous studies revealed that FGF signaling at the PSM regulates the wavefront position during somitogenesis. FGF modulates somite size by impeding maturation of PSM (Dubrulle et al., 2001; Sawada et al., 2001; Delfini et al., 2005; Wahl et al., 2007). Blocking FGF signaling increases somite length, while activating signaling has the opposite effect (Sawada et al., 2001). In addition, activation of FGF signaling blocks convergence movements and extends somite width (Furthauer et al., 1997; Krens et al., 2008). It is important to define regulators of FGF signaling in the PSM in order to determine how precise positional cues within the PSM are generated.

Here, we demonstrate that ChCh and Sip1a modulate FGF signaling in the PSM during somitogenesis. Surprisingly, we find that ChCh and Sip1 repress FGF expression. During somitogenesis, knockdown of *chch* or *sip1a* results in somites that are less extended thru anterior-posterior (A/P) axis while they are over-extended thru mediolateral axis. We also found that inhibition of ChCh and Sip1a perturbs oscillating gene expression in the forming somites. In ChCh or Sip1 compromised embryos, *fgf8* expression in the paraxial mesoderm

is expanded rostrally leading to altered somite size. Manipulations that reduced FGF8 signaling in ChCh and Sip1a compromised embryos restored somite size. This demonstrated that ChCh and Sip1a regulate somite morphogenesis by limiting FGF signaling. Together, these findings establish a novel role for ChCh as a repressor of FGF signaling.

Results

Role of ChCh and Sip1 in somitogenesis

In a previous study, we observed that ChCh is required for proper somite formation (Londin et al., 2007b). However, the mechanism of action of ChCh in somitogenesis is unknown. To investigate the function of ChCh in zebrafish somitogenesis, we inhibited ChCh activity using two translation blocking morpholinos (*chch* ATG MO and MO2) (Londin et al., 2007b). Microinjection of *chch* ATG MO presents a similar, but stronger somite phenotype than that produced by *chch* ATG MO2 microinjection. *chch* morpholino injected embryos are morphologically indistinguishable from control morpholino injected siblings until 75–95% epiboly stage (Fig 1B, C). Dorsal views of the 12-somite stage *chch* morphants reveals that somites are less extended thru anterior-posterior axis while they are over-extended thru mediolateral axis (Fig. 1K–M, 52%, n= 128). Moreover, these embryos have a shorter and wider body axis (Fig. 1 G, L; H, M). At 24 hours post fertilization, somites in ChCh compromised embryos are enlarged and lack their characteristic chevron shape (Fig. 1Q). Furthermore, although roughly 30 pairs of somites are formed in wild type siblings, *chch* morphants only form 22–26 somites (Fig. 1Q and data not shown). Taken together, these results demonstrate that ChCh is required during somitogenesis.

Because ChCh activity is mediated by Sip1 during gastrulation (Sheng et al., 2003) and homozygous *Sip1* knockout mice have a somite phenotype similar to *chch* morphants (Maruhashi et al., 2005), we asked whether Sip1 inhibition produced similar somite defects in zebrafish. Zebrafish have two *sip1* genes (*sip1a* and *sip1b*) (Delalande et al., 2008). To investigate the function of Sip1 in zebrafish somitogenesis, we inhibited Sip1 activity using previously characterized *sip1a* and *sip1b* morpholinos (Delalande et al., 2008). The *sip1a* ATG MO injected embryos have a somite phenotype similar to *chch* MO injected embryos, but the overall phenotype is more severe (Fig. 1I, N (89%, n=112) and data not shown). As in *chch* morphants, the somites are shorter thru anterior-posterior axis and over-extended thru mediolateral axis (Fig. 1N). Microinjection of *sip1a* splice morpholino also produced embryos were also short in anterior-posterior axis and elongated in the mediolateral axis (Fig. 1 J, O). Similar to *chch* morphants, somites are enlarged and lost their characteristic chevron shape at 24 hpf (Fig. 1R, S). Because this morpholino alters mRNA structure, we were able to monitor the effectiveness of the knockdown on eliminating wild-type mRNA (Supp. Fig. 1). Until dome stage, only wild-type mRNA is detected, which is presumably maternal message that is unaltered by the splice morpholino. Beginning at dome stage (4.3 hpf), the smaller misspliced product is detected. By 75% epiboly (8 hpf), no wild-type mRNA is apparent.

An alternatively spliced form of *sip1a* that lacks a portion of exon 8 has been described (Delalande et al., 2008). The alternative splice form lacks one zinc finger that is present in the longer form (Supp Fig. 2, blue bar, Supp Fig. 3A, dark blue box). We identified a similar alternatively spliced form of Sip1b that contains a deletion of 66 bp of exon 8 (Supp. Fig. 2). Since both *sip1a* and *sip1b* contained forms that lack the same region, we sought to determine whether either form of *sip1a* was required for somite formation. Both *sip1a* forms were detected by RT-PCR during a series of stages spanning the first 24 hpf (data not shown). We designed morpholinos to target the exon 8/intron 8 boundary (*sip1a* splice MO2, Supp Fig. 3A, pink bar) to drive production of the shorter form and a morpholino (*sip1a* splice MO3, Supp Fig. 3A, orange bar) that targets the alternative splice site in exon 8

and blocks production of the shorter form (leaving only the long form). Analysis of cDNA from embryo injected with each morpholino revealed that *sip1a* splice MO2 efficiently altered splicing so that only the shorter form was produced, while *sip1a* splice MO3 eliminated the shorter form (Supp. Fig. 3B, C). Somitogenesis was not altered by microinjection of either morpholino (data not shown). Due to toxic effects of co-injecting high doses of the two morpholinos (10 ng each), we were unable to analyze the effects of blocking production of both the long and short Sip1a forms in the same embryos. However, these experiments suggest that each Sip1a form is likely sufficient for normal somite development.

In a previous report, *sip1b* morphants were reported to have severe defects and produce only a few somites (Delalande et al., 2008). We observed a more severe phenotype than Delalande et. al. when we microinjected low doses of *sip1b* MO (data not shown). Therefore, we were unable to address the role of *sip1b* in somite formation using morpholino approaches.

ChCh and Sip1a are required for patterning of presomitic mesoderm

During somitogenesis, a series of highly regulated morphogenetic processes produce periodic and symmetrically formed somite boundaries. To characterize the origin of the severe somite defects in ChCh and Sip1a-compromised embryos, we performed a series of RNA *in situ* hybridizations with 14 somite stage *chch* and *sip1a* MO injected embryos. Since somites are derived from paraxial mesoderm cells, we analyzed the state of the presomitic mesoderm cells in ChCh and Sip1a compromised embryos. *papC* encodes a structural transmembrane protein and regulates the mesodermal segmentation during zebrafish development. In wild-type control embryos, four *papC* expression stripes corresponds to the (prospective) somites at the segmentation plate (Yamamoto et al., 1998), Fig. 2A). However, in *chch* and *sip1a* morphants, the number of stripes ranges from 5–8 (Fig. 2B, C). Moreover, tail bud expression domain of *papC* in ChCh and Sip1a compromised embryos is much broader mediolaterally than in wild type siblings (Fig. 2A–C).

Rostrocaudal polarity of the somites is also disrupted in ChCh and Sip1a compromised embryos. The segmental expression of myogenic regulatory factor *myoD* in the posterior half of the somites (Weinberg et al., 1996) is extended in the mediolateral axis (Fig. 2D–F). On the other hand, expression of *ephB2* (Durbin et al., 1998) (Fig. 2G–I), *dld* (Jiang et al., 2000; Holley et al., 2002) (Fig. 2J–L) and *fgf8* (Fig. 3 G–I) in the anterior half of the somites is reduced and expression is no longer restricted to the anterior region of the somites in both *chch* and *sip1a* morphants. Therefore, we conclude that rostrocaudal somite polarity requires ChCh and Sip1.

Inhibition of ChCh and Sip1a alters periodic gene expression

The “clock and wavefront” model describes the timing and positioning of somite boundaries during segmentation of the mesoderm (Cooke, 1978; Palmeirim et al., 1997; Forsberg et al., 1998; McGrew et al., 1998; Jiang et al., 2000; Bessho et al., 2001). In this model, somite size is the synchronous function of frequency of “molecular clock” oscillations and of the pace of “wavefront” progression. In *chch* and *sip1a* morphants, formed somites are smaller thru anterior-posterior axis. Either a faster ticking “molecular clock” or slowed down “wavefront” progression during somitogenesis can trigger reduction in somite size.

To test whether cyclic gene expression is altered in ChCh and Sip1a compromised embryos, we assayed *her1* and *her7* expression by RNA *in-situ* hybridization. *her1* and *her7* are both the output of the “molecular clock” and have characteristic 1 to 2 stripe expression domain

in the PSM at 10 somite stage (Fig. 3A,D) (Oates and Ho, 2002). However, the number of stripes observed in the ChCh and Sip1a compromised embryos ranged from 3 to 5 (Fig. 3A–C; D–F, marked with asterisks) indicating that impeding ChCh or Sip1a averts the proper termination of cyclic *her1* and *her7* expression in the anterior PSM. However, the performance and pace of the “molecular clock” is not substantially altered because despite the size difference, duration of somite formation in ChCh and Sip1a compromised embryos is comparable to control morpholino injected siblings (Supp Fig 4 and data not shown).

Failure to properly terminate *her1* and *her7* cyclic expression in the anterior PSM can be the result of slowed wavefront progression because the “wavefront” facilitates the transition of the PSM cells from the immature state to mature state by arresting the oscillating *her1* and *her7* wave. If the pace of the wavefront progression is slower, the overall rate of maturation of the PSM and therefore arresting the expression of cyclic *her1* and *her7* expression would also be slowed.

FGF signaling at the PSM is required for the regulation of the position of the wavefront during somitogenesis (Dubrulle et al., 2001; Sawada et al., 2001; Delfini et al., 2005; Wahl et al., 2007). A threshold level of FGF signaling facilitates the transition of the PSM cells from the immature state to mature state (Dubrulle et al., 2001; Sawada et al., 2001). Ectopic activation of the FGF signaling in zebrafish by surgically inserting FGF8 soaked beads in one side of the PSM gives rise to narrower somites in the region anterior to the FGF bead, while blocking FGF signaling has the opposite effect. On the FGF8 soaked bead implanted side, *her1* expression domain also extends more anteriorly than the control side (Sawada et al., 2001).

To determine whether the somite alterations in *chch* or *sip1* morphants are associated with altered *fgf8* gene expression, we assayed *fgf8* expression in these embryos by *RNA in-situ hybridization*. In both *chch* and *sip1a* ATG morpholino injected embryos, *fgf8* expression domain is expanded rostrally and extends into the midline and sometimes the (putative) somitic mesoderm (Fig. 3G–I). This suggests that the progression of the wavefront is much slower in ChCh and Sip1a compromised embryos. Slowing the wavefront is predicted to result in a broader zone of immature PSM. A similar phenomenon was also observed in *Sip1a* knockout mice (Maruhashi et al., 2005)

Rostral expansion of *fgf8* expression domain at tailbud can be explained by local changes in cell number in the PSM. We tested whether rate of cell proliferation is also altered in ChCh and Sip1a compromised embryos using cell proliferation marker anti-phosphorylated histone H3 antibody. There is no significant difference between ChCh or Sip1a compromised embryos and their wild type siblings (n= 29, 31 and 19 respectively, data not shown). This indicates that rostral expansion of *fgf8* expression domain is not due to altered cell proliferation.

The effects of ChCh knockdown on somite morphology are due to expanded FGF8 activity

In ChCh or Sip1a compromised embryos, *fgf8* expression in the paraxial mesoderm is expanded rostrally and somites are narrower at the A/P axis and wider in the mediolateral axis. We hypothesized that the expansion in FGF8 expression in these embryos caused alterations in somite morphology. To test that hypothesis, we determined the effects of *chch* and *sip1a* knockdown on embryos with compromised FGF signaling. If rostral expansion of *fgf8* is the cause of the somite phenotype observed in ChCh or Sip1a compromised embryos, then reduction of FGF8 activity will restore wild-type somite morphology. We employed two means to attenuate FGF activity, microinjection *sprouty4* (*spry4*) mRNA and *acerebellar* (*fgf8/ace*) mutant embryos.

spry4 is a feedback induced antagonist of FGF signaling. FGF8 induces *spry4* expression which in turn inhibits FGF activity (Furthauer et al., 2001). Microinjection of *spry4* sense RNA weakly impedes FGF8 signaling in zebrafish (Furthauer et al., 2001). Injection of *spry4* sense RNA into *chch* ATG morphants reduced the number of embryos with narrowed somites from 58% (*ChCh* ATG MO+*lacZ*) to 45% (*ChCh* ATG MO+*spry4* RNA) ($p = 0.0063$) (Supp. Fig. 5). Similarly, injection of *spry4* sense RNA into *sip1a* ATG morphants reduced the number of embryos with narrowed somites from 93% (*sip1a* ATG MO+*lacZ*) to 66% (*sip1a* ATG MO+*spry4* RNA) ($p = 0.0044$) (Supp. Fig. 5). The ability of *spry4* to restore somite morphology in only a subset of embryos likely reflect the poor stability of the injected RNA (Furthauer et al., 2001).

To circumvent this difficulty, we assayed the effects of blocking ChCh and Sip1a in *ace/FGF8* mutants (Reifers et al., 1998; Draper et al., 2001). *ace* mutants show a loss of the isthmus and cerebellum, but do not have overt somite defects due to redundant FGF activity (Reifers et al., 1998; Sawada et al., 2001). Injection of *chch* ATG MO into *ace* homozygous embryos (somite length = $47.4 \mu\text{m} \pm 2.4$, $n = 15$, $p = 0.003$) did not produce the alterations in somite morphology observed in control morpholino injected embryos (somite length = $48.1 \mu\text{m} \pm 1.4$, $n = 20$). In the same experiments, *chch* morpholino injection decreased somite length in wild type (somite length = $41.5 \mu\text{m} \pm 4.6$, $n = 32$) and *ace* heterozygous siblings (somite length = $40.4 \mu\text{m} \pm 2.4$, $n = 29$) (Fig. 4A).

Similarly, injection of *sip1a* ATG MO into *ace* homozygous embryos did not result in significant narrowing of somites in the A/P axis (somite length = $47.1 \mu\text{m} \pm 2.4$, $n = 9$, $p < 0.0001$) compared to control-injected embryos (somite length = $49.0 \mu\text{m} \pm 2.1$, $n = 22$). In the same experiments, somite length was decreased in *sip1a* ATG MO injected wild type (somite length = $40.1 \mu\text{m} \pm 2.7$, $n = 17$) and *ace* heterozygous siblings (somite length = $41.3 \mu\text{m} \pm 2.3$, $n = 16$).

These findings suggest that the consequences of *chch* knockdown on somite size are largely due to expansion of FGF signaling. However, in Sip1a compromised embryos, the overall phenotype is more severe than Chch compromised embryos and reduction of FGF signaling in these embryos is not sufficient to fully rescue the defects. Since Sip1 has wide range of functions that are distinct from known roles for ChCh including regulation of TGF- β and BMP pathways (Remacle et al., 1999; Verschuere et al., 1999; Postigo, 2003; Postigo et al., 2003; Nitta et al., 2004; van Grunsven et al., 2007) and cell fate determination (Remacle et al., 1999; Verschuere et al., 1999) some of the phenotypes observed in *sip1a* morphants may be due to FGF-independent activities of Sip1a.

Somite defects in *ace* mutants are unaltered by ChCh knockdown

Previous studies have demonstrated the ChCh is an effector of FGF signaling. However, our results reveal that ChCh also represses *fgf8* expression. FGF signaling in the somites is required to induce *myoD* expression and terminal differentiation of subset of fast muscle cells. *ace* mutants have reduced somatic *myoD* expression (Groves et al., 2005). If FGF8 functions downstream of ChCh in somitogenesis, somite defects present in *ace* mutants will not be altered by *chch* knockdown. Therefore, we performed RNA *in-situ* hybridization with *myoD* probe on ChCh compromised *ace* mutant embryos. As expected, we observed that lateral *myoD* expression in the somites is lost in *ace* mutant embryos, but adaxial cell expression was unaffected (Groves et al., 2005) (Fig. 5C). We observed similar reduction of *myoD* expression in ChCh compromised *ace*^{-/-} embryos as in control MO injected *ace*^{-/-} embryos (Fig. 5D). This observation is consistent with the model that FGF8 acts downstream of ChCh during somite formation.

To determine whether ChCh and Sip1a modulate FGF signaling in other tissues, we examined the consequence of knockdown of ChCh and Sip1a in the isthmus, which is a well-characterized site of FGF activity. We also observed that the expression of the FGF target gene *pax2a* is expanded anteriorly in the isthmus in *chch* morphants, but not in *sip1a* morphants (Fig. 6A–C). While the hindbrain is wider in ChCh and Sip1a compromised embryos (probably due to convergence defects), a similar alteration was not observed in *krox20* expression (Fig. 6D–F). These results suggest that negative regulation of FGF8 by ChCh is not limited to the mesoderm, but that the ChCh has a broader function in modulating FGF signaling.

Discussion

ChCh and Sip1 modulate FGF-dependent processes and act as a switch between mesodermal and neural inducing activities of FGF in chick, *Xenopus* and zebrafish (Sheng et al., 2003; Londin et al., 2007b). Although their regulatory properties and function during gastrulation have been studied extensively, very little is known about the requirements for ChCh and Sip1a at other stages. In zebrafish, both genes are expressed in the developing mesoderm (Londin et al., 2007a; Delalande et al., 2008). Previous studies using SIP1 knockout mice and *sip1* morphant zebrafish embryos did not clearly identify the function of Sip1 in somitogenesis (Maruhashi et al., 2005; Delalande et al., 2008).

In the present study, we characterized the function of ChCh and Sip1a in zebrafish somitogenesis. Our data revealed that *chch* and *sip1a* knockdown resulted in embryos with somites that are less extended thru A/P axis while over-extended in the mediolateral axis. In addition, cyclic expression of *her1* and *her7* is maintained in formed somites in these embryos. We observed that these defects correlated with an anterior expansion of FGF8 expression in the tailbud. In ChCh morphants, the defects in somite morphology could almost entirely suppressed by blocking FGF8, while the same treatment only partially restored the overall defects in *sip1a* morphants. Taken together, these findings demonstrate that ChCh and Sip1a regulate somitogenesis by mediating the position of the FGF8 mediated wavefront in the zebrafish PSM.

Expanded FGF8 expression in PSM would be predicted to alter the FGF gradient that regulates somite length (Sawada et al., 2001). However, our finding that somite width was also altered by the enhanced FGF8 expression was surprising. Because expression of dominant-negative ChCh blocks FGF mediated mesoderm induction in animal cap assays (Sheng et al., 2003), ChCh is generally thought of as a positive effector of FGF signaling. ChCh is induced in response to FGF in chick, *xenopus* and zebrafish (Sheng et al., 2003; Londin et al., 2007a) and our results demonstrate that ChCh represses expression of FGF8, implying that it functions in a negative feedback loop to repress FGF signaling. In a broad context, this relationship is consistent with functions of ChCh in cell movement. Previous studies have shown that ChCh impedes cell movement (Sheng et al., 2003; Londin et al., 2007b). While FGFs have complex roles in cell migration, in many tissues FGF promotes cell migration (Sun et al., 1999; Ciruna and Rossant, 2001; Yang et al., 2002). Therefore it is conceivable that in the effects of ChCh on cell movement are due to blocking, rather than promoting FGF signaling. Further studies are needed to elucidate the precise mechanisms by which ChCh modulates FGF signal transduction.

The somite phenotype observed in *sip1a* ATG morphants is stronger than *chch* ATG morphants and although somite phenotype can be rescued by blocking FGF activity, the overall defects cannot be fully restored. Thus far, Sip1 is the only described transcriptional target of ChCh. In several situations, overexpression of *sip1* is sufficient to compensate for ChCh deficits (Sheng et al., 2003; Snir et al., 2006). However, Sip1 has a wide range of

activities that are likely to be ChCh independent. These include regulation of TGF β pathways (Remacle et al., 1999; Verschueren et al., 1999; Postigo, 2003; Postigo et al., 2003), expression of BMP4 (Nitta et al., 2004; van Grunsven et al., 2007), mesodermal gene expression (Remacle et al., 1999; Verschueren et al., 1999) and E-cadherin transcription (Remacle et al., 1999; Comijn et al., 2001).

The functional differences between the alternatively spliced forms of zebrafish Sip1a remains unclear. The previously described alternatively spliced form of *sip1a* lacks a zinc finger (Delalande et al., 2008). Because we identified a structurally similar form of Sip1b (Supp. Fig. 2), we reasoned that the two forms have unique functions. To test for distinct activities during somitogenesis, we used splice morpholinos to block production of each form while leaving the other intact. Our approach demonstrated the effectiveness of morpholinos to specifically eliminate alternative spliced message. However, we were unable to detect somite defects or any other patterning defects in the respective Sip1a form-specific morphants. This suggests that each form can compensate for loss of the other during somitogenesis or that protein derived from maternal mRNA is sufficient to compensate for the loss of wild-type zygotic mRNA.

In conclusion, we studied the functions of ChCh and Sip1a during zebrafish somitogenesis and found that ChCh and Sip1a modulate somite morphogenesis by repressing FGF8 expression at the PSM. Significantly, we determined that Fgf8 is downstream of ChCh, suggesting a negative feedback loop between *chch/sip1a* and *fgf8*. Our data also demonstrates that regulation of FGF signaling by ChCh is not limited to the PSM. FGF signaling has diverse functions in a many biological processes and investigation of the vertebrate EST databases reveals that *ChCh* transcripts are detected in low levels in a wide array of tissues (data not shown). It will therefore be important for future studies to determine the importance of modulation of FGF signaling by ChCh in these contexts.

Experimental procedures

Adult fish and embryo maintenance

Adult zebrafish strains and embryos obtained from natural crossings were maintained at 28.5°C. Developmental stages of the embryos were determined according to Kimmel *et al.* (Kimmel et al., 1995).

Expression constructs, mRNA synthesis and morpholinos

spry4 ORF was amplified from 10 somite stage wild type total first strand cDNA using GTTCTAGAGGCTCGAGGAAGGTCCTGCAAACCAT/TCTTTTTGCAGGATCCTGAGGAACACGACCTACA primer pair. Amplified fragment is then cloned to pCS2+ at BamHI and XhoI sites. Capped sense mRNA was synthesized using mMMESSAGE mMACHINE Kit (Ambion).

The sequences of the morpholinos used are

chch ATG MO 5'- CAGTATAGTCCAGATCAGAAGACGC -3',

chch ATG MO2 5'- GCTTCTGGACACAACCGGTACACAT -3' (Londin et al., 2007b).

sip1a and *sip1b* ATG and splice morpholinos are kindly provided by Iain T. Shepherd (Delalande et al., 2008).

sip1a splice variant targeting MO2 5'- GTCTAAATGTGATATACCTGTGC -3'

sip1a splice variant targeting MO3 5'- CGCGTACATACCACTTTCAGTCTTC -3'

Primers used to monitor the efficiency of the splice variant targeting MO are:

MO2: ATGTACGCGTGTGACTTGTG / CATTTGTCGCACTGGTAAGG

MO3: TTAAGAAGACTGAAAGTGGAAAGC / CATTTGTCGCACTGGTAAG

Standard control oligo (Gene Tools) is used as control. mRNA and morpholino solutions were diluted to desired concentration with 0.2M KCl supplemented with phenol red. Typically, 500 pg of *spry4* mRNA, 10–15ng of *ChCh* ATG morpholino1 and *ChCh* ATG morpholino2, 2–4ng of *sip1a* ATG, 10ng of *sip1a* splice morpholino, 5ng of *sip1b* ATG, 1ng of *sip1b* splice morpholino is injected to one- to two-cell stage embryos.

Whole mount in-situ hybridization and immunohistochemistry

In situ hybridizations were performed according to Thisse *et al.* (Thisse *et al.*, 1993). Digoxigenin labeled probes for *in situ* hybridization was synthesized using T7, T3 or Sp6 RNA polymerase (Roche). Hybridized probes were detected using NBT/BCIP system (Roche). Stained embryos were re-fixed in 4% PFA and either stored in 100% methanol or cleared in Benzyl benzoate/benzyl alcohol solution (2:1) and mounted in Canada balsam/methyl salicylate (2.5% v/v) or flat mounted in 70% glycerol. Embryos were viewed with Zeiss Axioplan microscope, digitally photographed with Zeiss AxioCam camera. Images were processed and assembled with Zeiss Axiovision and Adobe Photoshop.

Genotyping *acerebellar (ace)* mutants

chch and *sip1a* ATG MO injected embryos obtained from *ace* heterozygous incross were genotyped following imaging. PCR primers to genotype *ace* embryos are GCCAAGCTTATAGTAGAGAC/ AAGTGATGACTTTTTTCAGATA. Following PCR, products were cut with EcoRV which digests the mutant but not wild-type alleles.

Supplementary Material

Refer to Web version on PubMed Central for supplementary material.

Acknowledgments

We thank Bernadette Holdener, Jerry Thomsen and members of their laboratories for helpful suggestions; Laura Mentzer for technical support; Heena Rana and Andrew Taibi for fish care. We are also grateful to the many labs that provided reagents including fish stocks, constructs and probes. This work was supported by NIH grant RO1HD043998 (HS).

References

- Amaya E, Musci TJ, Kirschner MW. Expression of a dominant negative mutant of the FGF receptor disrupts mesoderm formation in *Xenopus* embryos. *Cell*. 1991; 66:257–270. [PubMed: 1649700]
- Aulehla A, Wehrle C, Brand-Saberi B, Kemler R, Gossler A, Kanzler B, Herrmann BG. Wnt3a plays a major role in the segmentation clock controlling somitogenesis. *Dev Cell*. 2003; 4:395–406. [PubMed: 12636920]
- Bessho Y, Sakata R, Komatsu S, Shiota K, Yamada S, Kageyama R. Dynamic expression and essential functions of *Hes7* in somite segmentation. *Genes Dev*. 2001; 15:2642–2647. [PubMed: 11641270]
- Borland CZ, Schutzman JL, Stern MJ. Fibroblast growth factor signaling in *Caenorhabditis elegans*. *Bioessays*. 2001; 23:1120–1130. [PubMed: 11746231]
- Bottcher RT, Niehrs C. Fibroblast growth factor signaling during early vertebrate development. *Endocr Rev*. 2005; 26:63–77. [PubMed: 15689573]
- Cinquin O. Understanding the somitogenesis clock: what's missing? *Mech Dev*. 2007; 124:501–517. [PubMed: 17643270]

- Ciruna B, Rossant J. FGF signaling regulates mesoderm cell fate specification and morphogenetic movement at the primitive streak. *Dev Cell*. 2001; 1:37–49. [PubMed: 11703922]
- Comijn J, Berx G, Vermassen P, Verschueren K, van Grunsven L, Bruyneel E, Mareel M, Huylebroeck D, van Roy F. The two-handed E box binding zinc finger protein SIP1 downregulates E-cadherin and induces invasion. *Mol Cell*. 2001; 7:1267–1278. [PubMed: 11430829]
- Cooke J. Somite abnormalities caused by short heat shocks to pre-neurula stages of *Xenopus laevis*. *J Embryol Exp Morphol*. 1978; 45:283–294. [PubMed: 670864]
- Cooke J, Zeeman EC. A clock and wavefront model for control of the number of repeated structures during animal morphogenesis. *J Theor Biol*. 1976; 58:455–476. [PubMed: 940335]
- Coumoul X, Deng CX. Roles of FGF receptors in mammalian development and congenital diseases. *Birth Defects Res C Embryo Today*. 2003; 69:286–304. [PubMed: 14745970]
- Dale JK, Maroto M, Dequeant ML, Malapert P, McGrew M, Pourquie O. Periodic notch inhibition by lunatic fringe underlies the chick segmentation clock. *Nature*. 2003; 421:275–278. [PubMed: 12529645]
- Dale KJ, Pourquie O. A clock-work somite. *Bioessays*. 2000; 22:72–83. [PubMed: 10649293]
- Delalande JM, Guyote ME, Smith CM, Shepherd IT. Zebrafish *sip1a* and *sip1b* are essential for normal axial and neural patterning. *Dev Dyn*. 2008; 237:1060–1069. [PubMed: 18351671]
- Delfini MC, Dubrulle J, Malapert P, Chal J, Pourquie O. Control of the segmentation process by graded MAPK/ERK activation in the chick embryo. *Proc Natl Acad Sci U S A*. 2005; 102:11343–11348. [PubMed: 16055560]
- Draper BW, Morcos PA, Kimmel CB. Inhibition of zebrafish *fgf8* pre-mRNA splicing with morpholino oligos: a quantifiable method for gene knockdown. *Genesis*. 2001; 30:154–156. [PubMed: 11477696]
- Dubrulle J, McGrew MJ, Pourquie O. FGF signaling controls somite boundary position and regulates segmentation clock control of spatiotemporal Hox gene activation. *Cell*. 2001; 106:219–232. [PubMed: 11511349]
- Durbin L, Brennan C, Shiomi K, Cooke J, Barrios A, Shanmugalingam S, Guthrie B, Lindberg R, Holder N. Eph signaling is required for segmentation and differentiation of the somites. *Genes Dev*. 1998; 12:3096–3109. [PubMed: 9765210]
- Forsberg H, Crozet F, Brown NA. Waves of mouse Lunatic fringe expression, in four-hour cycles at two-hour intervals, precede somite boundary formation. *Curr Biol*. 1998; 8:1027–1030. [PubMed: 9740806]
- Furthauer M, Reifers F, Brand M, Thisse B, Thisse C. *sprouty4* acts in vivo as a feedback-induced antagonist of FGF signaling in zebrafish. *Development*. 2001; 128:2175–2186. [PubMed: 11493538]
- Furthauer M, Thisse C, Thisse B. A role for FGF-8 in the dorsoventral patterning of the zebrafish gastrula. *Development*. 1997; 124:4253–4264. [PubMed: 9334274]
- Furthauer M, Van Celst J, Thisse C, Thisse B. Fgf signalling controls the dorsoventral patterning of the zebrafish embryo. *Development*. 2004; 131:2853–2864. [PubMed: 15151985]
- Gates MA, Kim L, Egan ES, Cardozo T, Sirotkin HI, Dougan ST, Lashkari D, Abagyan R, Schier AF, Talbot WS. A genetic linkage map for zebrafish: comparative analysis and localization of genes and expressed sequences. *Genome Res*. 1999; 9:334–347. [PubMed: 10207156]
- Giudicelli F, Lewis J. The vertebrate segmentation clock. *Curr Opin Genet Dev*. 2004; 14:407–414. [PubMed: 15261657]
- Groves JA, Hammond CL, Hughes SM. Fgf8 drives myogenic progression of a novel lateral fast muscle fibre population in zebrafish. *Development*. 2005; 132:4211–4222. [PubMed: 16120642]
- Holley SA, Geisler R, Nusslein-Volhard C. Control of *her1* expression during zebrafish somitogenesis by a delta-dependent oscillator and an independent wave-front activity. *Genes Dev*. 2000; 14:1678–1690. [PubMed: 10887161]
- Holley SA, Julich D, Rauch GJ, Geisler R, Nusslein-Volhard C. *her1* and the notch pathway function within the oscillator mechanism that regulates zebrafish somitogenesis. *Development*. 2002; 129:1175–1183. [PubMed: 11874913]

- Huang H, Lu FI, Jia S, Meng S, Cao Y, Wang Y, Ma W, Yin K, Wen Z, Peng J, Thisse C, Thisse B, Meng A. *Amotl2* is essential for cell movements in zebrafish embryo and regulates c-*Src* translocation. *Development*. 2007; 134:979–988. [PubMed: 17293535]
- Jiang YJ, Aerne BL, Smithers L, Haddon C, Ish-Horowicz D, Lewis J. Notch signalling and the synchronization of the somite segmentation clock. *Nature*. 2000; 408:475–479. [PubMed: 11100729]
- Kimelman D, Maas A. Induction of dorsal and ventral mesoderm by ectopically expressed *Xenopus* basic fibroblast growth factor. *Development*. 1992; 114:261–269. [PubMed: 1374313]
- Kimmel CB, Ballard WW, Kimmel SR, Ullmann B, Schilling TF. Stages of embryonic development of the zebrafish. *Dev Dyn*. 1995; 203:253–310. [PubMed: 8589427]
- Krens SF, He S, Lamers GE, Meijer AH, Bakkers J, Schmidt T, Spaik HP, Snaar-Jagalska BE. Distinct functions for ERK1 and ERK2 in cell migration processes during zebrafish gastrulation. *Dev Biol*. 2008; 319:370–383. [PubMed: 18514184]
- LaBonne C, Whitman M. Mesoderm induction by activin requires FGF-mediated intracellular signals. *Development*. 1994; 120:463–472. [PubMed: 8149921]
- Lee BM, Buck-Koehntop BA, Martinez-Yamout MA, Dyson HJ, Wright PE. Embryonic neural inducing factor *chur* is not a DNA-binding zinc finger protein: solution structure reveals a solvent-exposed beta-sheet and zinc binuclear cluster. *J Mol Biol*. 2007; 371:1274–1289. [PubMed: 17610897]
- Londin ER, Mentzer L, Gates KP, Sirotkin HI. Expression and regulation of the zinc finger transcription factor *Churchill* during zebrafish development. *Gene Expr Patterns*. 2007a; 7:645–650. [PubMed: 17521969]
- Londin ER, Mentzer L, Sirotkin HI. *Churchill* regulates cell movement and mesoderm specification by repressing Nodal signaling. *BMC Dev Biol*. 2007b; 7:120. [PubMed: 17980025]
- Maruhashi M, Van De Putte T, Huylebroeck D, Kondoh H, Higashi Y. Involvement of SIP1 in positioning of somite boundaries in the mouse embryo. *Dev Dyn*. 2005; 234:332–338. [PubMed: 16127714]
- McGrew MJ, Dale JK, Fraboulet S, Pourquie O. The lunatic fringe gene is a target of the molecular clock linked to somite segmentation in avian embryos. *Curr Biol*. 1998; 8:979–982. [PubMed: 9742402]
- Nitta KR, Tanegashima K, Takahashi S, Asashima M. *XSIP1* is essential for early neural gene expression and neural differentiation by suppression of BMP signaling. *Dev Biol*. 2004; 275:258–267. [PubMed: 15464588]
- Oates AC, Ho RK. Hairy/E(spl)-related (*Her*) genes are central components of the segmentation oscillator and display redundancy with the Delta/Notch signaling pathway in the formation of anterior segmental boundaries in the zebrafish. *Development*. 2002; 129:2929–2946. [PubMed: 12050140]
- Palmeirim I, Henrique D, Ish-Horowicz D, Pourquie O. Avian hairy gene expression identifies a molecular clock linked to vertebrate segmentation and somitogenesis. *Cell*. 1997; 91:639–648. [PubMed: 9393857]
- Postigo AA. Opposing functions of ZEB proteins in the regulation of the TGFbeta/BMP signaling pathway. *Embo J*. 2003; 22:2443–2452. [PubMed: 12743038]
- Postigo AA, Depp JL, Taylor JJ, Kroll KL. Regulation of Smad signaling through a differential recruitment of coactivators and corepressors by ZEB proteins. *Embo J*. 2003; 22:2453–2462. [PubMed: 12743039]
- Pourquie O. Vertebrate somitogenesis. *Annu Rev Cell Dev Biol*. 2001; 17:311–350. [PubMed: 11687492]
- Pourquie O. The segmentation clock: converting embryonic time into spatial pattern. *Science*. 2003; 301:328–330. [PubMed: 12869750]
- Prince VE, Holley SA, Bally-Cuif L, Prabhakaran B, Oates AC, Ho RK, Vogt TF. Zebrafish lunatic fringe demarcates segmental boundaries. *Mech Dev*. 2001; 105:175–180. [PubMed: 11429294]
- Qiu X, Xu H, Haddon C, Lewis J, Jiang YJ. Sequence and embryonic expression of three zebrafish fringe genes: lunatic fringe, radical fringe, and manic fringe. *Dev Dyn*. 2004; 231:621–630. [PubMed: 15376327]

- Reifers F, Bohli H, Walsh EC, Crossley PH, Stainier DY, Brand M. Fgf8 is mutated in zebrafish acerebellar (ace) mutants and is required for maintenance of midbrain-hindbrain boundary development and somitogenesis. *Development*. 1998; 125:2381–2395. [PubMed: 9609821]
- Remacle JE, Kraft H, Lerchner W, Wuytens G, Collart C, Verschuere K, Smith JC, Huylebroeck D. New mode of DNA binding of multi-zinc finger transcription factors: deltaEF1 family members bind with two hands to two target sites. *Embo J*. 1999; 18:5073–5084. [PubMed: 10487759]
- Saga Y, Takeda H. The making of the somite: molecular events in vertebrate segmentation. *Nat Rev Genet*. 2001; 2:835–845. [PubMed: 11715039]
- Sato Y, Yasuda K, Takahashi Y. Morphological boundary forms by a novel inductive event mediated by Lunatic fringe and Notch during somitic segmentation. *Development*. 2002; 129:3633–3644. [PubMed: 12117813]
- Sawada A, Shinya M, Jiang YJ, Kawakami A, Kuroiwa A, Takeda H. Fgf/MAPK signalling is a crucial positional cue in somite boundary formation. *Development*. 2001; 128:4873–4880. [PubMed: 11731466]
- Serth K, Schuster-Gossler K, Cordes R, Gossler A. Transcriptional oscillation of lunatic fringe is essential for somitogenesis. *Genes Dev*. 2003; 17:912–925. [PubMed: 12670869]
- Sheng G, dos Reis M, Stern CD. Churchill, a zinc finger transcriptional activator, regulates the transition between gastrulation and neurulation. *Cell*. 2003; 115:603–613. [PubMed: 14651851]
- Snir M, Ofir R, Elias S, Frank D. *Xenopus laevis* POU91 protein, an Oct3/4 homologue, regulates competence transitions from mesoderm to neural cell fates. *Embo J*. 2006; 25:3664–3674. [PubMed: 16858397]
- Sun X, Meyers EN, Lewandoski M, Martin GR. Targeted disruption of Fgf8 causes failure of cell migration in the gastrulating mouse embryo. *Genes Dev*. 1999; 13:1834–1846. [PubMed: 10421635]
- Sutherland D, Samakovlis C, Krasnow MA. branchless encodes a *Drosophila* FGF homolog that controls tracheal cell migration and the pattern of branching. *Cell*. 1996; 87:1091–1101. [PubMed: 8978613]
- Takada S, Stark KL, Shea MJ, Vassileva G, McMahon JA, McMahon AP. Wnt-3a regulates somite and tailbud formation in the mouse embryo. *Genes Dev*. 1994; 8:174–189. [PubMed: 8299937]
- Thisse B, Thisse C. Functions and regulations of fibroblast growth factor signaling during embryonic development. *Dev Biol*. 2005; 287:390–402. [PubMed: 16216232]
- Thisse C, Thisse B, Schilling TF, Postlethwait JH. Structure of the zebrafish snail1 gene and its expression in wild-type, spadetail and no tail mutant embryos. *Development*. 1993; 119:1203–1215. [PubMed: 8306883]
- van Grunsven LA, Taelman V, Michiels C, Verstappen G, Souopgui J, Nichane M, Moens E, Opdecamp K, Vanhomwegen J, Kricha S, Huylebroeck D, Bellefroid EJ. XSip1 neuralizing activity involves the co-repressor CtBP and occurs through BMP dependent and independent mechanisms. *Dev Biol*. 2007; 306:34–49. [PubMed: 17442301]
- Verschuere K, Remacle JE, Collart C, Kraft H, Baker BS, Tylzanowski P, Nelles L, Wuytens G, Su MT, Bodmer R, Smith JC, Huylebroeck D. SIP1, a novel zinc finger/homeodomain repressor, interacts with Smad proteins and binds to 5'-CACCT sequences in candidate target genes. *J Biol Chem*. 1999; 274:20489–20498. [PubMed: 10400677]
- Wahl MB, Deng C, Lewandoski M, Pourquie O. FGF signaling acts upstream of the NOTCH and WNT signaling pathways to control segmentation clock oscillations in mouse somitogenesis. *Development*. 2007; 134:4033–4041. [PubMed: 17965051]
- Weinberg ES, Allende ML, Kelly CS, Abdelhamid A, Murakami T, Andermann P, Doerre OG, Grunwald DJ, Riggleman B. Developmental regulation of zebrafish MyoD in wild-type, no tail and spadetail embryos. *Development*. 1996; 122:271–280. [PubMed: 8565839]
- Yamamoto A, Amacher SL, Kim SH, Geissert D, Kimmel CB, De Robertis EM. Zebrafish paraxial protocadherin is a downstream target of spadetail involved in morphogenesis of gastrula mesoderm. *Development*. 1998; 125:3389–3397. [PubMed: 9693142]
- Yang X, Dormann D, Munsterberg AE, Weijer CJ. Cell movement patterns during gastrulation in the chick are controlled by positive and negative chemotaxis mediated by FGF4 and FGF8. *Dev Cell*. 2002; 3:425–437. [PubMed: 12361604]

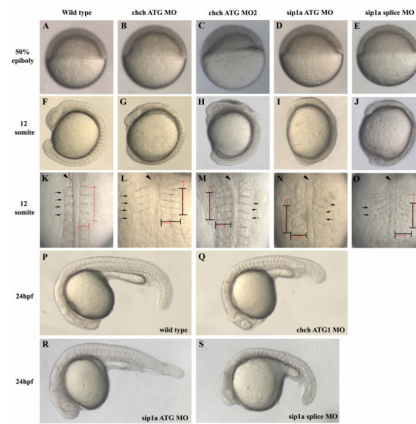


Figure 1. ChCh and Sip1a are required for somitogenesis

Living wild-type, ChCh and Sip1a-compromised embryos. Early epiboly movements appear normal in *chch* or *sip1a* morphants (A–E). By 12s misshapen somites are apparent in both *chch* and *sip1a* morpholino treated embryos (F–J). In these embryos, somites are less extended thru anterior-posterior axis and over-extended thru mediolateral axis (K–O). Horizontal and vertical red dotted lines span the width and length of the first four wild type somites for comparison to the first four somites of morphant embryos, which are marked with a black line (K–O). At 24hpf, somites are enlarged and misshapen in both ChCh and Sip1a compromised embryos (P–S). Arrowheads denote notochord and black arrows denote somites. (A–J, P–S) are lateral views; (K–O), dorsal views.

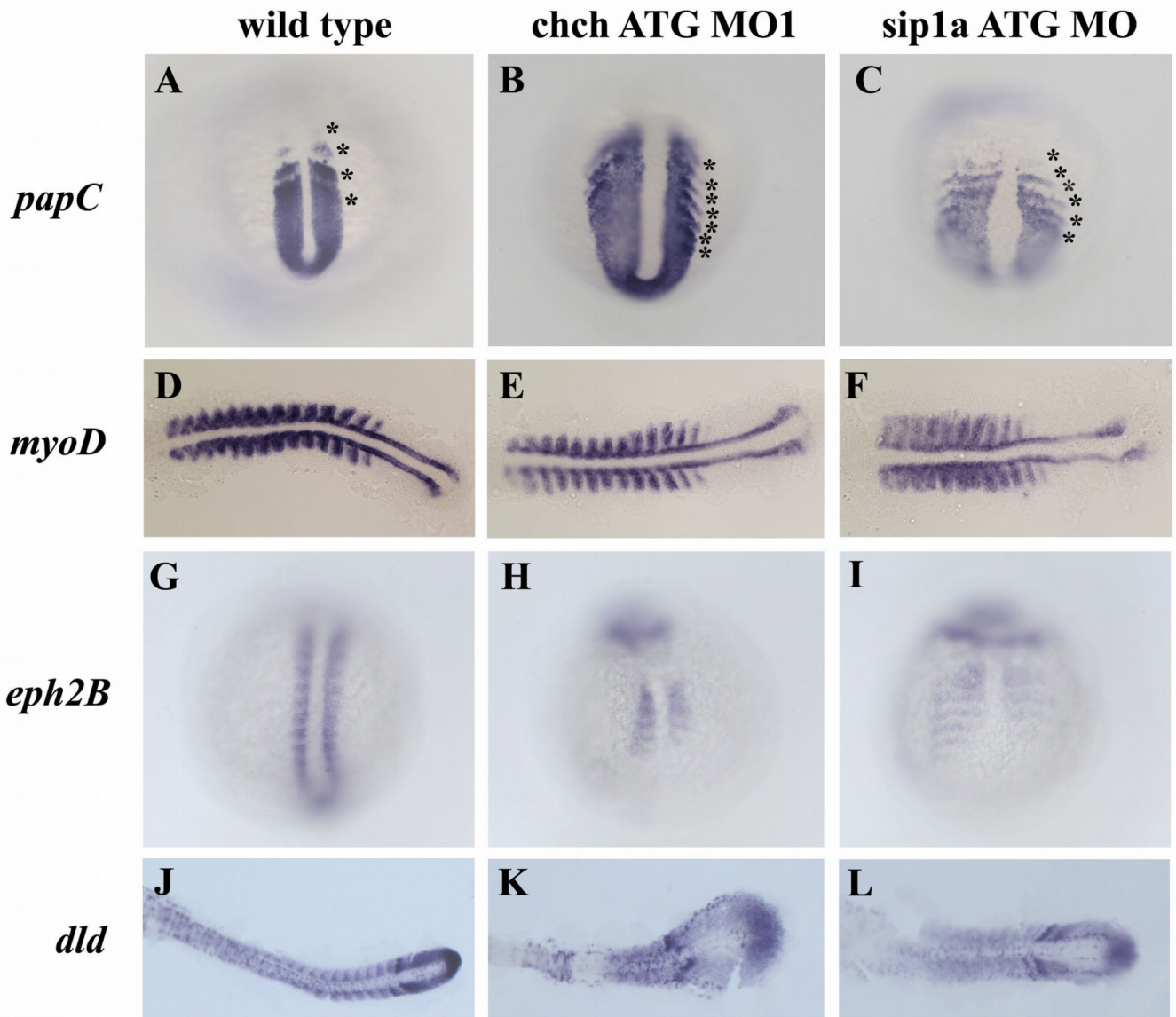


Figure 2. Patterning of the presomitic and somitic mesoderm is disrupted in ChCh and Sip1a compromised embryos

Whole mount (A–C, G–I) and flat mount (D–F, J–L) RNA *in situ* hybridization of somite markers in wild type, ChCh and Sip1a compromised embryos. All views are dorsal; anterior to the top (A–C, G–I) and anterior to the left (D–F, J–L)). The expression domains of the PSM marker, *papC* is broader mediolaterally in ChCh and Sip1a compromised embryos than the wild type siblings (A–C). The number of the *papC* expression stripes corresponding to the prospective and formed somites at the segmentation plate in *chch* and *sip1a* MO is higher than in wild type siblings (A–C, compare asterisks number). The myogenic regulatory factor, *myoD*, is expressed in the posterior somite compartment in *chch* and *sip1a* MO injected embryos as in wild-type embryos (D–F). *eph2B* and *dld* expression at the anterior half of the somites (G–L) is reduced and diffuse. Asterisks denote (prospective) somites.

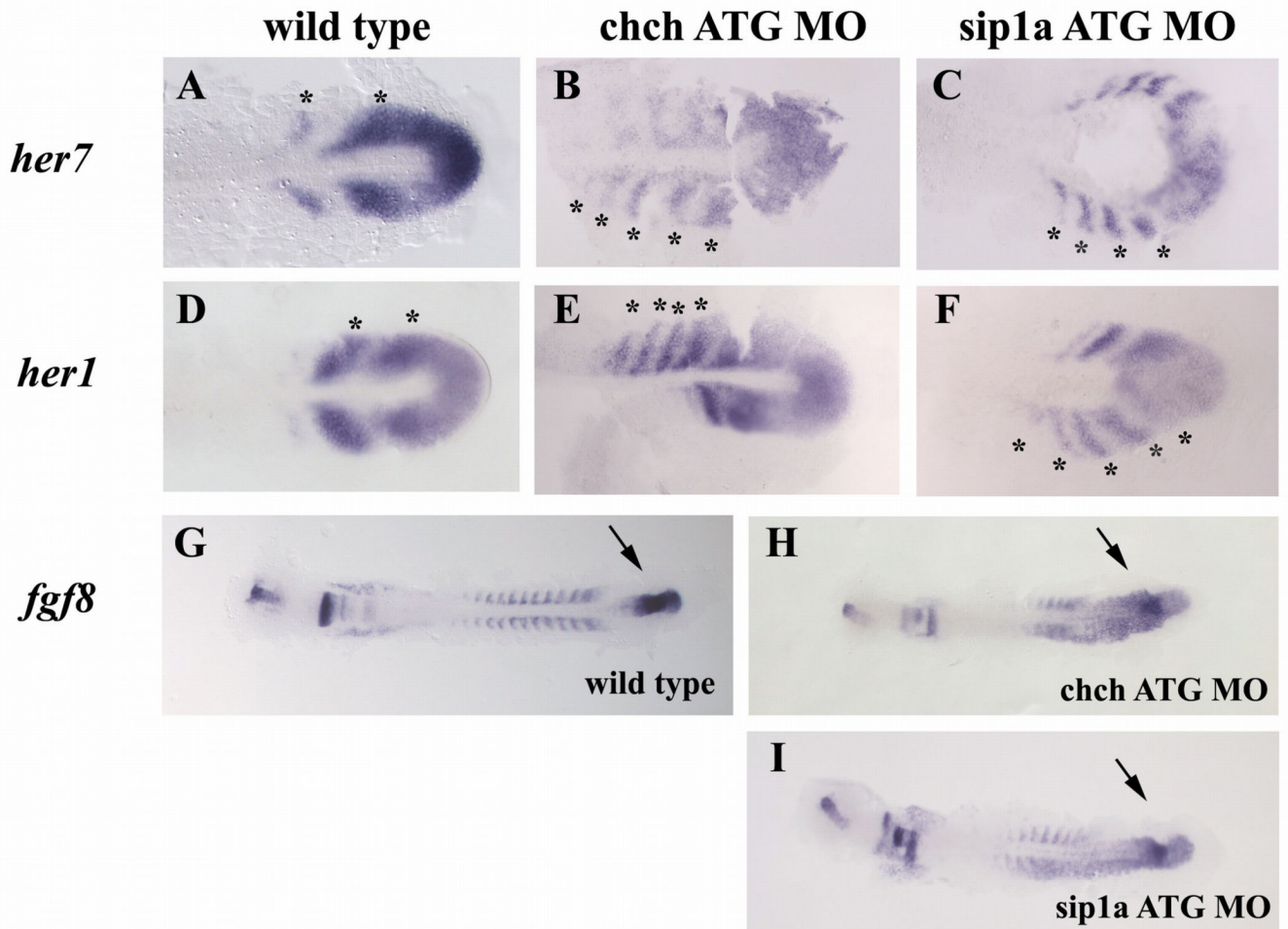


Figure 3. Inhibition of ChCh and Sip1a affects the components of the “clock and wavefront model”

Flat mount RNA *in situ* hybridization of 10 somite stage wild type, ChCh and Sip1a compromised embryos (A–I). All views are dorsal; anterior to the left. In wildtype embryos, periodic activation of Notch signaling provides cycling gene expression of Notch pathway genes such as *her1* and *her7* (A–F). The number of the *her7* expressing stripes in *chch* and *sip1a* ATG MO injected embryos ranges from 4 to 5 (B,C; E,F). *fgf8* expression domain at tailbud is expanded anteriorly in ChCh and Sip1a compromised embryos (G–I). Asterisks denote each *her1* or *her7* expressing premesoderm stripe (A–F). Arrows denotes *fgf8* tailbud expression domain (G–I).

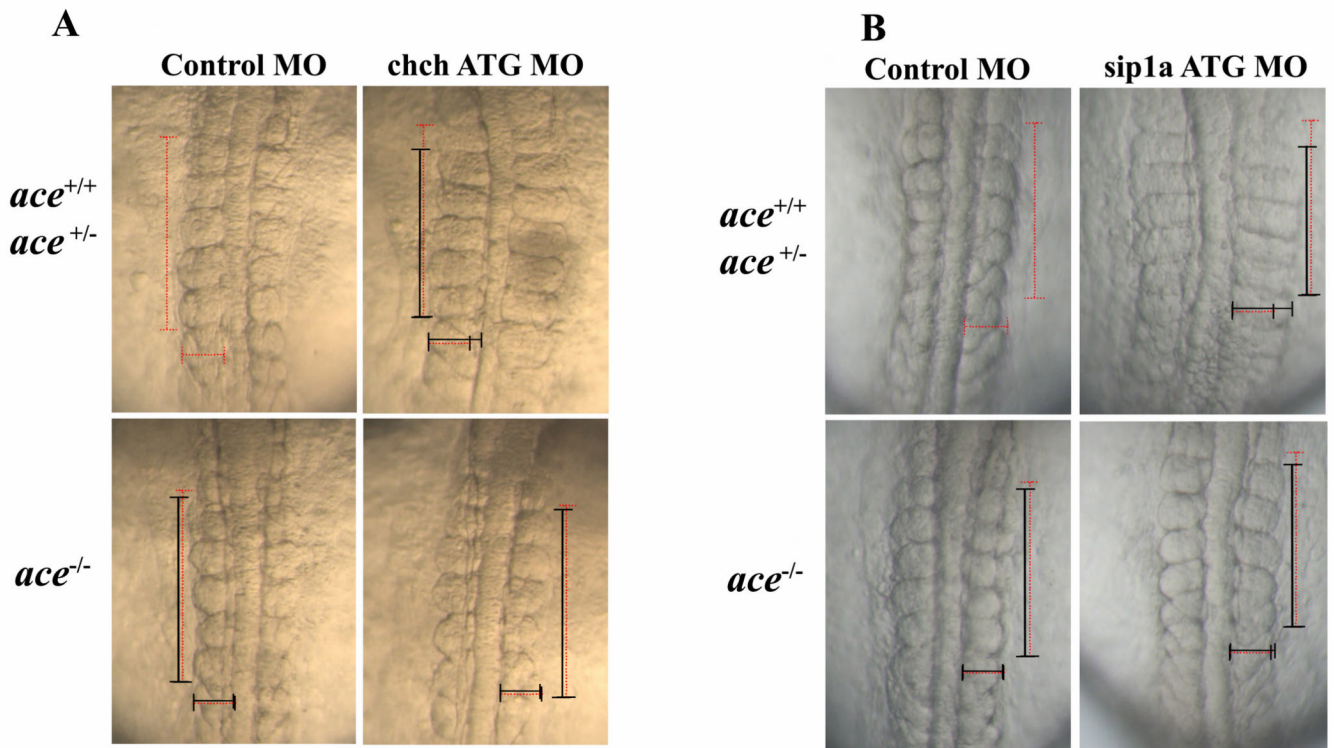


Figure 4. Somite malformation in ChCh and Sip1a compromised embryos can be rescued by reduction of FGF8

(A) Dorsal views of 10 somite stage and (B) 12 somite stage living embryos, anterior to the top. Somites are narrower at A/P axis, broader at mediolateral axis in wild type and *ace* heterozygous *chch* morphants, but not *ace* homozygous *chch* morphants (A). *ace* homozygous *sip1a* ATG morphants does not have somite phenotype but wild type and *ace* heterozygous *sip1a* morphants still have the somite defects. (B). Horizontal and vertical red dotted line spans the first five somites of the control injected embryo width and length for comparison to the first five somite of morphant embryos which is indicated with a black line. Embryos were genotyped for the *ace* allele after imaging.

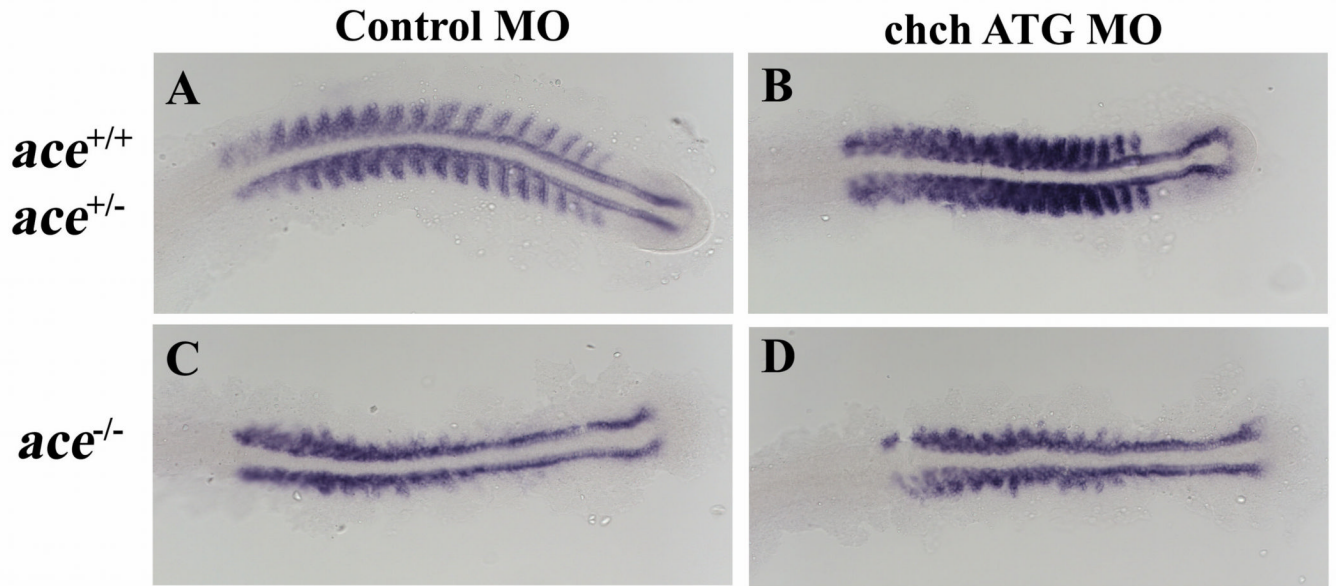


Figure 5. Somite defects in *ace* mutants are unaltered by ChCh knockdown

Flat mount RNA in situ hybridization of *myoD* in 17 somite stage ChCh compromised wild type, *ace*^{+/-} and *ace*^{-/-} embryos (A–D). All views are dorsal; anterior to the left. Lateral *myoD* expression in the somites is lost in *ace* mutant embryos (C). *myoD* expression pattern in ChCh compromised *ace*^{-/-} embryos is similar to control MO injected *ace*^{-/-} siblings (D).

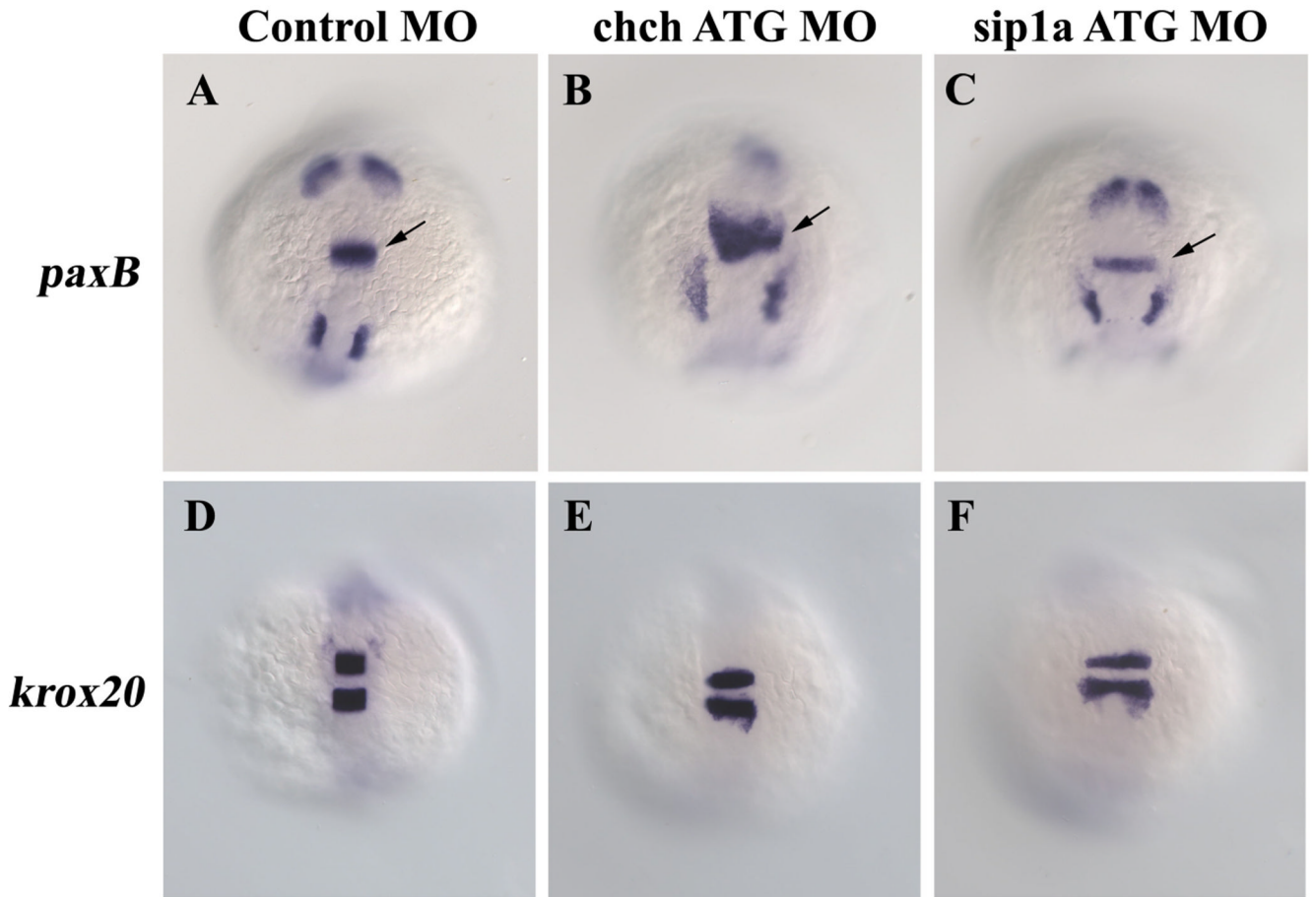


Figure 6. Repression of FGF8 by ChCh is not limited to the mesoderm

Whole mount RNA *in situ* hybridization of *pax2a* and *krox20* in 10-somite stage ChCh and Sip1a compromised embryos (A–F). All views are dorsal; anterior to the top. FGF target gene *pax2a* is expanded anteriorly in the isthmus in *chch* morphants, but not in *sip1a* morphants (A–C). The anterior extent of *krox20* expression is not altered by *chch* or *sip1a* knockdown (D–F). Arrows denote isthmus.